



Novel Biorenewable Composites Based on Poly (3-hydroxybutyrate-co-3-hydroxyvalerate) with Natural Fillers

Stanislaw Kuciel¹ · Karolina Mazur¹ · Paulina Jakubowska²

Published online: 7 February 2019
© The Author(s) 2019

Abstract

Due to the ubiquity and single-use character of plastic products, their production represents a burden to the environment. Therefore, an increasing interest in biodegradable and bio-compostable materials has been observed in the recent years. Bio-based materials are becoming more and more popular, especially in applications where biodegradability provides an advantage for customers and environment. However, biodegradable materials are more expensive compared with durable plastic materials, so to reduce costs and in order to improve their mechanical properties, biocomposites are created by reinforcement with natural fibers: cellulose, hemp, jute, cotton, etc. This paper is focused on the investigation of the selected group of biocomposites based on poly (3-hydroxybutyrate-co-3-hydroxyvalerate) with the addition of 15 wt% of various fillers (nanocellulose, walnut shell flour, eggshell flour, and tuff). Thus far, there is limited information concerning comparison of the different natural fillers introduced into the poly(3-hydroxybutyrate-co-3-hydroxyvalerate) matrix. Here, the following mechanical properties were evaluated: the tensile strength, modulus of elasticity, strain at break, flexural modulus, and flexural stress at 3.5% strain. The tensile test was performed at various temperatures (− 24, + 23, and + 60 °C), followed by samples conditioning in water and compost. Thermal behavior of the biocomposites was studied by means of differential scanning calorimetry (DSC) and thermogravimetric analysis (TGA). The study showed that the value of the elasticity modulus of each composite was higher in comparison with neat poly (3-hydroxybutyrate-co-3-hydroxyvalerate), at each of the above temperatures. The factor responsible for the enhancement of the mechanical properties of composites (enhancement of the stiffness of the material) was the increase in crystalline phase content in composites. Interestingly, at − 24 °C, all of the analyzed composites exhibited over twofold increase in tensile strength which was accompanied by an almost 30% increase in elastic modulus. This phenomenon likely resulted from an increase in tensile strength and an increase in internal stress at interfaces within the components of the composites during tests. It was also observed that both conditioning in water and degradation in the compost heap led to a considerable decrease in mechanical properties of the examined composites. The scanning electron microscopy analysis, carried out to assess the distribution of particles and the adhesion of fillers to the matrix, revealed that the size and the shape of the particles affected the mechanical properties of the composites.

Keywords Poly (3-hydroxybutyrate-co-3-hydroxyvalerate) · Nanocellulose · Walnut shell flour · Eggshell flour · Tuff · Polymer-matrix composites (PMCs)

Introduction

Due to the omnipresence and disposable character of plastic products, it is very difficult to reduce their production, which is an issue for solid waste management. Therefore, the increased interest in biodegradable and biocompostable materials has been exhibited both by researchers and entrepreneurs in the recent years. Usually, biodegradable materials are used to produce surgical implants in vascular applications, or orthopaedic equipment. They are also used as devices for the controlled release of drugs, or as absorbable

✉ Stanislaw Kuciel
stask@mech.pk.edu.pl

¹ Institute of Material Engineering, Faculty of Mechanical Engineering, Cracow University of Technology, Cracow, Poland

² Institute of Technology and Chemical Engineering, Faculty of Chemical Technology, Poznan University of Technology, Poznan, Poland

sutures [1]. Biodegradable polymers are divided mainly into two groups: polyesters and polyglycols. The most popular materials from these groups are most known polylactide (PLA) and polyhydroxyalkanoates (PHA) [1, 2]. However, because PLAs degrade slower than the PHAs, PHAs attract more attention regarding the production of disposable products [3]. PHAs are a family of fully biodegradable polyesters. They are produced by microorganisms through the fermentation of carbon-containing sources [4]. Physical properties of PHAs are comparable with other polyesters, for instance, PLA, polyglycolic acid (PGA), and polycaprolactone (PCL). Products made of plastic in conditions of normal operation (contact with the atmosphere) are characterized by high durability. However, after the required cycle life, PHBV based products can be subjected to hydrolytic and/or biological degradation, eventually transforming into H_2O , CO_2/CH_4 and biomass. The products of this process are practically non-harmful to the environment (water, biomass) while carbon dioxide or methane can be used as fuel in power plants. Owing to excellent biocompatibility and biodegradability of PHAs, they can be used in medical applications, tissue engineering, and drug delivery [5].

Unfortunately, the high costs of production of biodegradable polymers still hamper their industrial application. In order to reduce the above costs and improve their mechanical properties, biodegradable polymers are increasingly combined with natural fillers [6]. The addition of natural fillers to the polymer matrix enhances the mechanical and thermal properties, increases stiffness as well as flexibility during the processing [7]. It can also ameliorate the ability of a given material to degrade (into carbon dioxide/methane, water, and/or various inorganic compounds) under the influence of the particular conditions or enzymatic action of bacteria and other living organisms [8, 9]. It is worth mentioning that there are many studies on plastic biodegradable composites reinforced with natural fillers e.g., sisal, cellulose, hemp, jute, cotton, pineapple, etc. [10–13].

By contrast, until recently little attention was paid to the biocomposites based on PHAs, which is likely related to their high production costs, difficult processing, and slow crystallization rate [14, 15]. The research concerning the PHA polymers is typically focused on the general reduction of their undesirable brittleness and optimization of processing parameters with the particular emphasis put on polyhydroxybutyrate (PHB) and poly(hydroxybutyrate-co-hydroxyvalerate) PHBV [16].

In general, in biocomposites reinforced with natural fillers, elastic modulus increases, but a decrease of tensile strength may be observed. For instance, Srubar et al. [17] investigated composites based on PHBV with the addition of oak wood flour (OWF), with fiber loads varying between 8.4 and 36.2 vol.%. In their study, there was decreased in tensile strength from 34.8 ± 0.7 MPa in the neat PHBV, to

21.4 ± 1.8 MPa (36.2 vol%) in composites. Furthermore, nearly linear increase in Young's modulus in the dependency with the increasing fiber load was observed. The modulus amounted to $3\,800 \pm 102$ MPa in neat PHB, and to $4\,820 \pm 180$ MPa in PHB composites with the addition of 36.2 vol.% of OWF fibers.

Similar results were obtained by Gunning et al. [18], who manufactured biocomposites based on PHB with the addition of 10–30 wt.% of fillers such as hemp, jute and lyocell fibers. The decrease in tensile strength in comparison with neat PHBV was observed for all the examined composites. In that study, the value of flexural modulus increased, whereby the composites with 30 wt% of jute fiber content exhibited the highest increase to almost 4000 MPa (591% in comparison with neat PHB).

Analysis of hydrolytic degradation is important for biomaterials, which can be used as implants elements. The degradation of PHBV depends on many factors such as the chain scission of PHBV ester groups via a random chain, and the strong electron-donating effect of substituent group of carbon atoms at α -position to the ester oxygen [19]. Hydrolytic degradation of PHBV was previously reported by Deroine et al. [20]. They performed accelerated aging in distilled water at 25, 30, 40 and 50 °C and noticed the increased in the temperature of the process and the increased in water sorption by 0.8% (25/30 °C) up to 1.8% (50 °C) weight gain. Additionally, after 360 days of incubation in water (40 °C) the tensile strength decreased from 35 ± 1.2 MPa (unaged) to 26.5 ± 1 MPa.

Many studies confirmed that the addition of natural fillers to biocomposites accelerate the degradation process [2, 21]. Wu [22] studied PHA composites with the addition of 20 and 40 wt.% of tea plant fibers (TPF). The author ascertained that composites with natural fibers degrade more rapidly than neat polymers in soil compost. This degradation was confirmed by the increased weight loss of the PHA matrix as a function of incubation time. The higher content of fibers, the faster was the degradation. Additionally, the water resistance of PHA/TPF (40 wt%) was lower than that of PHA/TPF (20 wt%). However, the biodegradability process can be also calculated from CH_4 production. Ryan et al. [23] investigated injection molded neat PHBV and composites with 20 wt.% of oak wood flour (P, P20), maleated PHBV (2M) and with 20 wt.% of OWF (2M20) and PHBV with 20 wt.% of silanated OWF (P20S). They measured biodegradability by mass loss and additionally by comparing the measured CH_4 production. They noticed that different compatibilization treatments and addition of WF affect the mass loss rate (R). The lowest R was observed for P and the higher for P20S.

The objective of this study was to produce composites based on biodegradable, thermoplastic polymer PHBV with the following natural fillers: nanocellulose (NC), walnut shell flour (WSF), eggshell flour (ESF) and tuff (T). The

values of mechanical properties, including tensile strength, modulus of elasticity, strain at break, flexural modulus, and flexural stress at 3.5% strain were measured. Thermal properties were also examined. Scanning electron microscopy (SEM) images were obtained to evaluate the distribution of particles and the adhesion of fillers in a matrix.

Methodology

Materials

PHBV copolymer (PHI001) provided by Nature Plast (France) in the form of pellets was used as a matrix. It is a biodegradable thermoplastic material intended mainly for injection molding. According to its technical data sheet, it melts at 160 °C and it has a density of 1.25 g/cm³.

The following additives were used as fillers:

- Nanocellulose (NC) (ARBOCEL UFC 100 BRIGHT), produced by J. Rettenmaier and Söhne (Rosenberg, Germany). This material is “ready-to-use” for direct processing by virtue of extrusion plants and injection molding machinery and its particle size varies between 5 and 13 μm.
- Walnut shell flour (WSF) (REHOFIX UNG 300), produced by J. Rettenmaier and Söhne. This material is “ready-to-use” natural filler that can be directly processed by means of extrusion facilities and injection molding machinery and its particle size varies between 170 and 230 μm.
- Eggshell flour (ESF), obtained from a chicken farm located in Poland (Sieslawice). The eggshells were ground with a Retsch ZM 200 (Haan, Germany) mill machine in the laboratory to obtain flat-shaped particles with the approximate size of 20–100 μm. The surface treatment of eggshells included the immersion in 10% NaOH solution for 30 min at room temperature (23 °C). Then the eggshell flour was rinsed three times with distilled water and subsequently subjected to drying in the thermal chamber (KC100), at 180 °C for 1 h.
- Tuff (T), delivered from a mine in Filipowice (Poland). The tuff from Filipowice is a solid pyroclastic rock, which consists mostly of such minerals as sanidine, kaolinite, illite, biotite, and quartz. Tuff is strongly alkaline, contains ~ 15 wt% of K₂O, while the amount of Na₂OH is low. Its oxide composition is shown in Table 1. The particles in the size range of 5–20 μm were obtained by

grinding using the Retach ZM 200 mill. After grinding, they were rinsed in 1 molar hydrochloric acid and then calcined at 800 °C.

Methods

Composites Preparation

Four types of composites were produced with equal fillers content (15 wt%). Firstly, in order to achieve a better homogenization of PHBV granules and different fillers before the injection took place, each composition had been subjected to the conventional dry mixing process carried out for 15 min.

Standard dumbbell samples with the dimension specified by the PN-EN ISO 3167, were manufactured using the KRAUSS MAFFEI KM40 (Eschweiler, Germany) injection molding machine (with a screw diameter of 25 mm and L/D ratio of 23), without previous extrusion and regranulation. The parameters of the injection process were the same for all of the tested materials: injection temperatures – 120 °C, 160 °C, 170 °C, and 175 °C; speed of screw rotation – 50 rpm; an injection time – 2 s; holding pressure time – 4 s; cooling time – 20 s; mould temperature 50 °C; hydraulic back pressure 8.5 MPa.

Properties of PHBV and its Composites

The density of the samples was measured by means of the immersion method according to the PN-EN 1936 standard using the RADWAG WAS 220/X electronic analytical balance (Birstall, United Kingdom).

Charpy impact test was carried out in accordance with PN-EN ISO 179-2 standard using Zwick/Roell MTS-SP (Ulm, Germany) testing machine. The average un-notched impact strength (a_{cU}) was calculated.

The morphology of each fiber in a matrix was studied using a scanning electron microscope JEOL 5510LV (Tokyo, Japan) low vacuum with an accelerating voltage of 5 and 10 kV the study concerned surface of the tensile on the tensile fracture samples, gold-sputtered before the SEM examination.

The mechanical properties (tensile and bending tests) were estimated by means of universal MTS Criterion Model 43 (Eden Prairie, USA) testing machine. The values were obtained from an average of at least 5 samples. The tensile test was performed with a constant cross-head speed of 5 mm/min and the elongation was evaluated using an

Table 1 Oxide composition of the tuff filler

Oxide composition	SiO ₂	Al ₂ O ₃	K ₂ O	CaO	Fe ₂ O ₃	MgO	TiO ₂	Na ₂ OH
[wt%]	56.04	16.73	15.01	5.39	5.38	0.6	0.85	0.39

MTS axial extensometer and crosshead displacement. The tensile test included the measurement of tensile strength, modulus of elasticity, and strain at break. It was carried out according to the PN-EN ISO 527-1:2012 standard [24] under the standard conditions (23 °C and 65% HR), and also at -24 and 60 °C, by putting the samples in the temperature chamber (Instron, Norwood, USA). The samples had been conditioned at the test temperature for 30 min before the tensile test was performed. The temperature range applied during the examination reflects the lowest and the highest temperatures at which PHBV can find its potential use bio-based materials are not only used in medicine, but also as automotive parts, where operating temperatures can vary from -40 °C (outdoor parking lots) up to 125 °C (under the hood) [25].

The flexural three-point bending test (flexural modulus and flexural stress at 3.5% strain) was carried out according to the PN-EN ISO 178 standard on the neat PHBV and its composites (23 °C and 65% HR), with a constant cross-head speed of 2 mm/min.

Thermogravimetric Analysis

Thermogravimetric analysis (TGA) was performed under nitrogen atmosphere in a NETSCH model TG 209 F3 instrument (Selb, Germany). The samples, weighing approximately 10 mg, taken from the central parts of the injection-molded specimens of standard dumbbell-shape, were placed in an Al₂O₃ crucible and heated at the temperature range varying from room temperature (23 °C) to 700 °C. The heating rate was kept at 10°C/min and a nitrogen gas flow rate at 30 ml/min. The derivative of TGA curves (DTG) was obtained using software dedicated to TA analysis.

Differential Scanning Calorimetry

Differential scanning calorimetry (DSC) was performed using a NETZSCH model DSC-200 with computer software for test analysis (Selb, Germany). The measurements were applied to the samples weighing 7–7.5 mg, taken from the central parts of the injection-molded specimens of standard dumbbell-shape. The examination took place at the temperatures range from -25 to 210 °C under argon atmosphere. All measurements were performed according to the following procedure: heating from -25 to 210 °C at a scanning rate of 10°C/min, keeping the material at 210 °C for 2 min and then cooling down from 210 to -25 °C at the scanning rate of 5°C/min. The whole process was carried out twice to eliminate the processing memory/history of the materials (the first heating-cooling cycle) and thermal properties of the composites (the second heating-cooling cycle). An empty pan was used as a reference.

In order to determine the effect of the used biofillers on the thermal properties of the polymer matrix, both the reference sample and all produced biocomposites were tested under the same conditions (according to the above-mentioned temperature program).

Melting parameters such as glass transition (T_g), melting temperature (T_m), melting enthalpy (ΔH_m), cold crystallization process (T_{cc}), cold crystallization enthalpy (ΔH_{cc}), and degree of crystallinity (X_c) were also determined. The degree of crystallinity of PHBV and PHBV composites was calculated with the following equation:

$$X_c = \frac{(\Delta H_m - \Delta H_{cc}) \cdot 100}{\Delta H_m^o \cdot w(\text{PHBV})} \quad (1)$$

where: ΔH_m is melting enthalpy (J/g), ΔH_{cc} is cold crystallization enthalpy (J/g), ΔH_m^o stands for the melting enthalpy of fully crystalline PHBV which equals to 146 J/g [26–28] and $w(\text{PHBV})$ is the weight fraction of PHBV in the sample.

All melting parameters obtained for biocomposites were then compared to those obtained for the polymer matrix.

Water Absorption

Water absorption was measured according to the PN-EN ISO 62:2000 standard. The samples were immersed in distilled water and maintained at 23 °C for 1, 7 and 21 days. Subsequently, they were dried and weighted with the accuracy of 0.0001 g. Each sample was measured three times. To determine the influence of water uptake on the basic mechanical properties of the test materials, samples incubated in water for 21 days were subjected to tensile tests.

Biodegradability

The biodegradability of the specimens was evaluated by measuring the changing weight of neat PHBV and its composites in the compost heap (85 wt% of natural soil, 10 wt% of leaves and 5 wt% of grass). The samples (standard dumbbell samples 10×4×150 mm) were completely buried for 21 and 49 days. The external conditions in which they underwent maturation were 60 °C and 80% HR. Prior to the mechanical tests, the retrieved samples were washed and dried with paper.

Results and Discussion

Mechanical Properties

In Table 2, symbols of all composites, density, and unnotched impact strength are presented. The density of the tested composites was at the same level, with the exception

Table 2 Symbols of composites, density and Charpy impact strength for neat PHBV and biocomposites

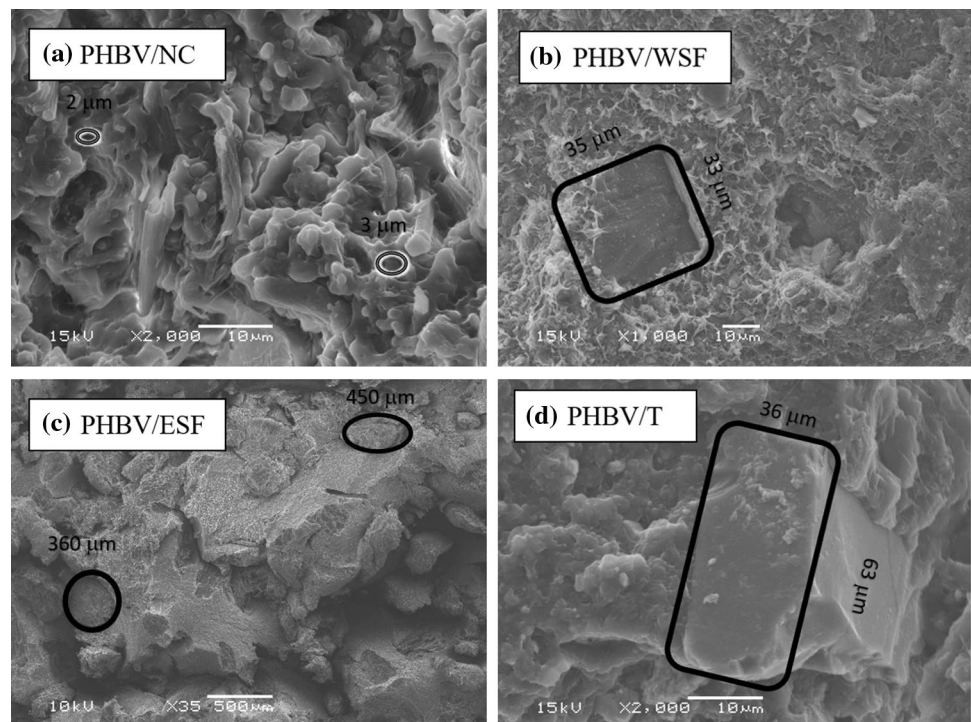
Sample	Composition	ρ [g/cm ³]	a_{cU} [kJ/m ²]
PHBV	Poly(3-hydroxybutyrate-co-3-hydroxyvalerate)	1.22 ± 0.002	8.1 ± 0.01
PHBV/NC	Poly(3-hydroxybutyrate-co-3-hydroxyvalerate) + 15 wt % nanocellulose	1.260 ± 0.002	3.5 ± 0.01
PHBV/WSF	Poly(3-hydroxybutyrate-co-3-hydroxyvalerate) + 15 wt % walnut shells flour	1.257 ± 0.006	2.9 ± 0.01
PHBV/ESF	Poly(3-hydroxybutyrate-co-3-hydroxyvalerate) + 15 wt %, egg shells flour	1.26 ± 0.021	5.3 ± 0.03
PHBV/T	Poly(3-hydroxybutyrate-co-3-hydroxyvalerate) + 15 wt % volcanic tuff	1.316 ± 0.001	6.1 ± 0.02

of PHBV/T, the density of which increased by approx. 5% compared with the neat PHBV. The impact strength of composites was primarily influenced by particle size, adhesion to the matrix and the uniformity of their distribution in the polymer composite. Large WSF particles of nearly 0.23 mm in size, with low adhesion to the hydrophobic matrix, and the smallest microcellulose particles, with a high tendency to agglomerate, reduced the impact strength of the tested composites. The developed surface of particles of mineral origin (porous tuff or egg shells) also led to much lower impact strength. The best results were noted for the biocomposites filled with volcanic tuff compared with pure PHBV, where the decrease in impact strength amounted to about 25%. However, the lowest impact strength was shown in the samples filled with WSF. In this case, the decrease in relation to the neat PHBV amounted to about 65%. The reduction of the impact strength was also observed in the

composites filled with lignocellulosis particles (NC and WSF). As regards the impact strength, the reduction level was two times higher compared with mineral particles. The addition of natural fillers to the polymers matrix had a negative side-effect i.e. increased brittleness, as demonstrated by impact tests [29].

Satisfactory mechanical properties of composite materials depend on strong adhesion between the phases and uniform distribution of all components in the matrix. Thus, SEM images were used to examine the morphology of individual fillers of composites and to assess their dispersion in the matrix as well as simply interfacial interactions between the matrix and fillers. Figure 1 a-d shows SEM images by used various ratio of magnification on tensile fracture samples.

As shown in Fig. 1a, small cellulose particles (5–13 μ m) were evenly distributed in the composite matrix. Good interfacial adhesion of the filler is visible. WSF particles

Fig. 1 The SEM images the of microstructure of PHBV composites **a** PHBV/NC, **b** PHBV/WSF, **c** PHBV/ESF, **d** PHBV/T

(170–230 μm) were much larger than cellulose particles, which led to poorer adhesion and contributed to more rapid degradation. Due to the fact that ESF particles have the form of a plate and their size is large (20–100 μm), their SEM images revealed some notable rifts which were possibly the remains of the filler. Leaving a trace on the polymer matrix, indicates low adhesion and the phenomenon known for typical fibers under the term “pull out”, in this case the dropping of filler particles from the polymer matrix. In the Fig. 1, both traces and single particles of WSF or ESF particles embedded in the polymer matrix can be observed. The weakest adhesion was, however, typical of the composites with the addition of tuff. In that case, the discontinuities between the matrix and the filler were clearly visible. SEM images stay in accordance with the results of mechanical tests, because the composites with lower adhesion tend to exhibit also lower mechanical properties [30].

Influence of Temperature

Figures 2, 3 and 4 show the comparison of tensile strength, modulus of elasticity, and elongation in the tested composites at temperatures $-24\text{ }^{\circ}\text{C}$, $+23\text{ }^{\circ}\text{C}$ and $+60\text{ }^{\circ}\text{C}$. The tensile strength decreased and elastic modulus increased at room temperature. This effect is very often described in reports concerning the composites that contain natural fillers [31–33]. The decrease in tensile strength is connected with the poor compatibility between the filler and the matrix and a weak adhesion between these two phases. The tensile strength properties determined at $-24\text{ }^{\circ}\text{C}$, showed over four-fold increase in tensile strength of the composites compared with them at elevated temperature (PHBV/WSF- 17.34 MPa

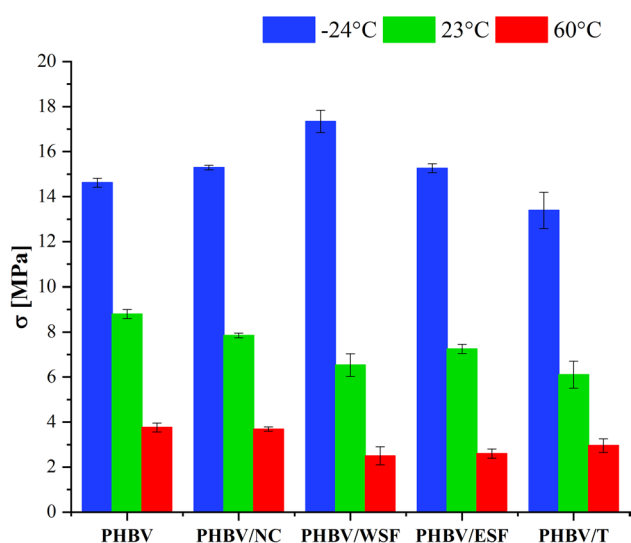


Fig. 2 Comparison of the tensile strength of neat PHBV and its bio-composites in various temperatures $-24\text{ }^{\circ}\text{C}$, $+23\text{ }^{\circ}\text{C}$, $+60\text{ }^{\circ}\text{C}$

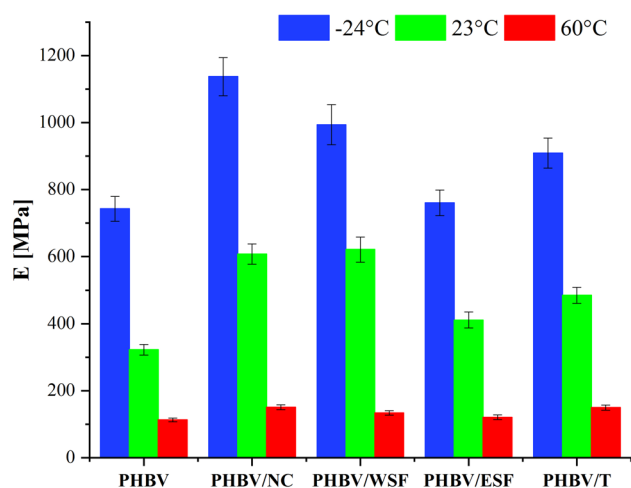


Fig. 3 Comparison of the modulus of elasticity of neat PHBV and its bio-composites in various temperatures $-24\text{ }^{\circ}\text{C}$, $+23\text{ }^{\circ}\text{C}$, $+60\text{ }^{\circ}\text{C}$

to 6.98 MPa), which results from the fact that the glass transition temperature for PHBV is at $-5\text{ }^{\circ}\text{C}$ [34].

The increase in elastic modulus compared with pure PHBV was observed for each type of filler at all three temperatures. The highest value of elastic modulus was recorded for PHBV/NC $-1,137 \pm 0.03\text{ MPa}$ (at $-24\text{ }^{\circ}\text{C}$), while the lowest for pure PHBV $112.8 \pm 0.04\text{ MPa}$ (at $+60\text{ }^{\circ}\text{C}$). Interestingly enough, all the composites exhibited nearly 30% increase in modulus of elasticity resulting from the addition of lignocellulose fillers and a slightly lower one stemming from the addition of mineral particles. This is probably due to an increase in tensile strength and an increase in internal stresses at the interfaces of the components of

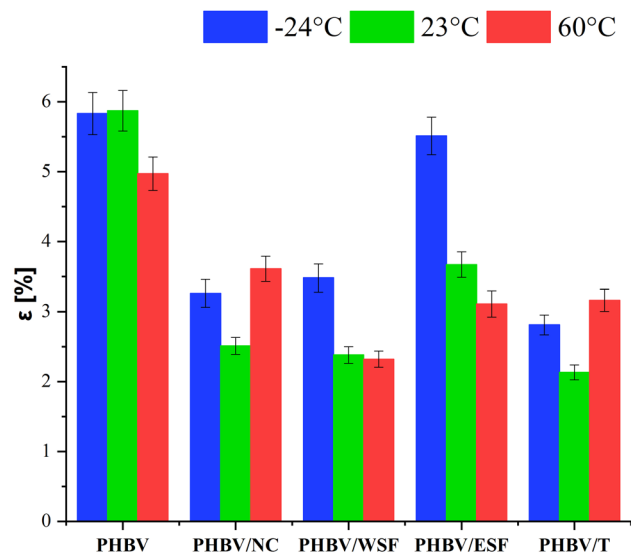


Fig. 4 Comparison of the strain at break of neat PHBV and its bio-composites in various temperatures $-24\text{ }^{\circ}\text{C}$, $+23\text{ }^{\circ}\text{C}$, $+60\text{ }^{\circ}\text{C}$

the composition during tests [35]. Stresses in the matrix are reinforced by stresses induced by fillers, which are arranged in a different direction in relation to the cross-section.

The deformation at break decreased by about 30% at each of the tested temperatures, for all the composites except of PHBV/ESF. Large lobular mineral of ESF particles likely allowed to maintain the deformation by means of resistance forces arising when they are removed from the polymer matrix.

Similar results for mechanical, thermo-mechanical, and morphological properties of the PHBV biocomposites filled with bamboo fibers (30 wt.% and 40 wt.%) were described by Singh et al. [36]. They observed an increase in the modulus of elasticity with the increasing fiber content. The modulus of elasticity increased by 67% for the composites with the addition of 30 wt% fibers and by 175% for those with the addition of 40 wt.% fibers. Such an increase of the modulus of elasticity can be attributed to a homogeneous dispersion of fibers in the PHBV matrix. Tensile strength of PHBV decreased with the increased content of bamboo fibers, which can be attributed to the lack of sufficient interaction between the fibers and the matrix. In addition, a comparative analysis was conducted between the PHBV-based biocomposites with the addition of bamboo and the PHBV-based biocomposites filled with wood fibers. Both types of fibers contributed to the increase in the elasticity modulus of the produced composites. Statistically, no influence of the fiber type on the mechanical properties of composites was found. Notch impact strength of PHBV decreased with the addition of the fibers and the reduction was higher for bamboo fiber composites. No impact of the fiber type on the thermal stability of the composites was observed but the addition of wood fibers resulted in a higher heat deflection temperature (HDT) compared to bamboo fibers.

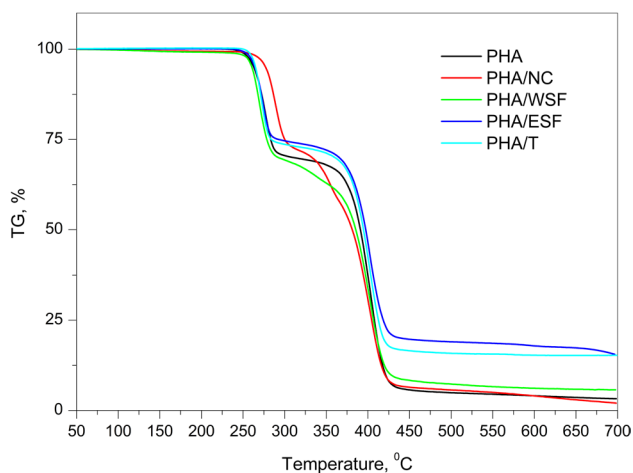


Fig. 5 TGA curves of the neat PHBV and its biocomposites

TGA Analysis

Thermogravimetric studies can help establish the boundary conditions for the processing of thermoplastic materials. This is particularly important for PHBV, which has a narrow processing window. TGA of the PHBV biocomposites was conducted to determine the impact of the filler concentration in the PHBV matrix (Fig. 5).

The value of initial degradation temperature (T_i) was equal to the temperature observed when the initial weight of the heated sample decreased by 2% (T_2) [28]. The study pertained also to another important thermal property, namely the correspondence between the applied temperature and the maximum rate of the weight loss (T_p), which is defined as the peak value of the first derivative (DTG) of the TGA curve (Fig. 6).

The temperature corresponding to the 2% weight loss (T_2) and that corresponding to the maximum rate of a weight loss (T_p) for PHBV and its biocomposites is essential for evaluating thermal stability. The values are summarized in Table 3.

The TGA curve for PHBV shows a gradual weight loss with the temperature increase, which started at about 250 °C, and a complete degradation at around 410 °C, leaving a weight residue of 3.22%. Thermal instability of PHBV above

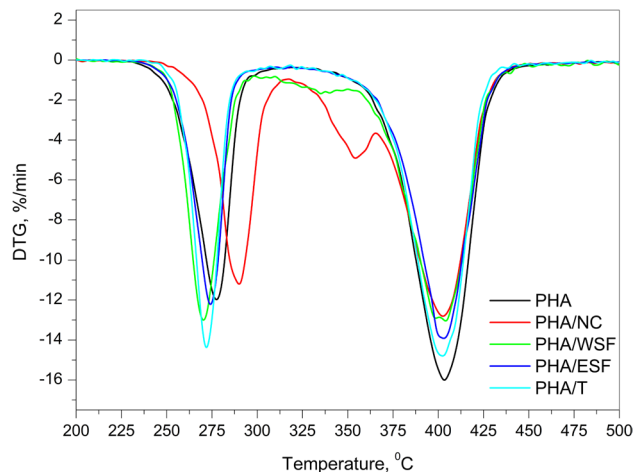


Fig. 6 DTG curves of the neat PHBV and its biocomposites

Table 3 An initial degradation temperature (T_2) and the temperature of maximum rate of weight loss (T_p) for PHBV and its composites

Material	$T_2/^\circ\text{C}$	$T_{p1}/^\circ\text{C}$	$T_{p2}/^\circ\text{C}$
PHBV	254.9	277.5	403.5
PHBV/NC	267.7	291.2	402.6
PHBV/WSF	253.1	271.3	403.2
PHBV/ESF	257.0	272.6	402.8
PHBV/T	259.2	272.4	402.7

250 °C has been reported in the previous works [37, 38]. It has been suggested that the degradation process involves the chain scission and hydrolysis, which lead to a reduction in molecular weight. PHBV thermally degrades to produce polymeric chains terminated with carboxyl and vinyl groups. Carboxyl end groups of polyester catalyze hydrolysis reaction. The processing temperature at 175 °C for the biocomposites used in this work is about 75 °C below the initial degradation temperature of the neat polymer.

The addition of biofillers to a PHBV matrix generally did not change thermal stability of the biocomposites. The analysis of the TGA and DTG curves revealed that the PHBV/WSF, PHBV/ESF and PHBV/T had similar characteristic degradation temperatures as PHBV, such as the temperature for 2% weight loss and that corresponding to the maximum rate of a weight loss, which appeared at about 250 (T_2), 275 (T_{p1} – the first step of degradation) and 400 °C (T_{p2} – the second step of degradation) (Table 3). A higher thermal stability was achieved only for the system filled with nanocellulose (PHBV/NC). In this case, an increase in T_2 by 12.8 and T_{p1} by 13.7 °C was noted, which is an increase of about 5% as compared to the neat PHBV.

DSC Analysis

The values of the melting parameters for PHBV (reference material) and for all composites with biofillers recorded in the second heating cycle are presented in Table 4. The DSC curves obtained for the tested materials in the second heating cycle are shown in Fig. 7.

In semicrystalline polymers, the crystallization behavior governs not only the crystalline structure and morphology, but also the final mechanical properties of the material. The PHBV is a semicrystalline polymer that can crystallize from either molten or glassy states, corresponding to melt crystallization and cold crystallization respectively [28]. It was reported that the crystallization of PHB is slow and incomplete, while its melting is complex due to superimposed melting – recrystallization – re-melting processes [39].

The analysis of DSC results proves that PHBV does not crystallize during the cooling step. These results suggest is the presence of some amount of other constituents in the matrix of PHBV, which impede the ability to crystallize. For all the samples, the DSC curves revealed similar

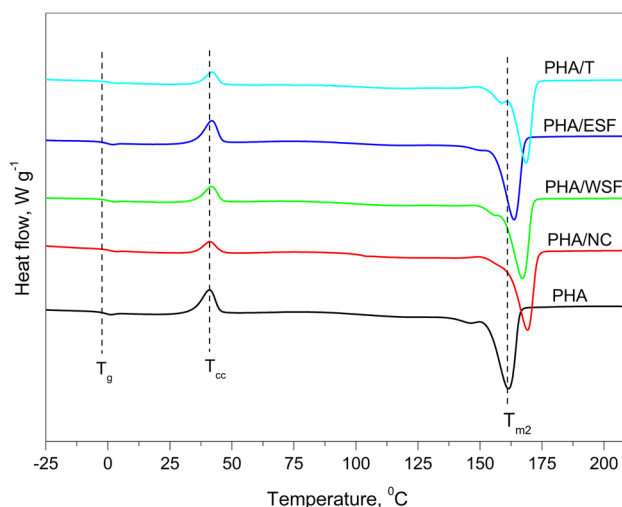


Fig. 7 DSC heating curves the of neat PHBV and its biocomposites in the second heating cycle

thermal events: the glass transition (characterized by T_g), cold crystallization process (characterized by T_{cc} and the cold crystallization enthalpy ΔH_{cc}), as well as the melting process (characterized by T_m and the melting enthalpy ΔH_m). The DSC curve corresponding to the second heating scan of PHBV showed a glass transition at about -1 °C, cold crystallization at 41 °C and a melting peak at about 160 °C. These values were similar to those reported in the literature [26, 27, 40–42]— T_m at about 160–180 °C.

The analysis of results of the second heating cycle showed that the introduction of the fillers to the PHBV matrix contributed to the increase of the glass transition, cold crystallization and melting temperature of the biocomposite in comparison with the reference sample.

The introduction of filler may increase or decrease T_g , but it may also have no effect on it. The relative density of both the amorphous and crystalline regions influences the degree of crystallinity and as a result, T_g can reach either higher or lower values [43]. The analysis of the glass transition temperatures of the composites showed an increase in the value of T_g compared to the reference materials from 0.6 °C for PHBV/ESF to 1.6 °C for PHBV/T. The determined melting temperatures of the analyzed composites were also elevated compared to PHBV. The second heating scan for

Table 4 Temperatures of glass transition (T_g), cold crystallization (T_{cc}), melting (T_m), cold crystallization enthalpy (ΔH_{cc}), melting enthalpy (ΔH_m) and degree of crystallinity (X_c) for tested materials

Material	$T_g/^\circ\text{C}$	$T_{cc}/^\circ\text{C}$	$T_m/^\circ\text{C}$	ΔH_{cc}	ΔH_m	$X_c/\%$
PHBV	-1.26	40.98	161.64	4.97	16.89	9.61
PHBV/NC	0.14	41.14	169.14	1.80	17.51	12.66
PHBV/WSF	0.03	41.80	167.13	3.09	18.12	12.11
PHBV/ESF	-0.71	41.81	163.80	4.51	19.70	12.24
PHBV/T	0.38	41.97	168.63	2.40	18.55	13.01

PHBV and PHBV composites included a small shoulder before the maximum peak. This behavior was attributed to the bimodal distribution of crystallite size resulting from changes in molecular weight due to random scission of long PHBV chains, i.e. to the decrease in the molecular weight. A similar process upon heating was reported by Tanase et. al [27] for the melting temperature of PHB/cellulose fiber and for PHB/PLA blend [8]. Furthermore, an increase in the value of T_m , compared to the reference materials, from 2.2 °C for PHBV/ESF to 7.5 °C for PHBV/NC was observed.

The melting enthalpy of all the tested biocomposites was higher in comparison to the melting enthalpy of neat PHBV, which indicated an interference of the biofillers with the crystalline structure of the polymer [44].

Simultaneously, it was also noted that the degree of crystallinity of biocomposites was also higher compared to the unmodified PHBV. It should be stressed that the increase in crystalline phase content in a composite is often responsible for enhancing mechanical properties of the material, as it provides physical crosslinking sites which enhance the stiffness of the material in a similar way as the chemical crosslinking density in thermoset resins [43]. The crystallization process is based on a competition between the nucleation effect and polymer chain mobility. An increase in crystallinity results from higher chain mobility and better packing of segments [37]. Data regarding X_c revealed that the addition of biofillers elevated this parameter from 9.6% for neat PHBV to up to 13.0% for PHBV/ESF composites (increase by 35.4%). The addition of other particulate biofillers also led to an increased crystallinity in comparison to PHBV, which amounted to 26.0% in the case of PHBV/NC, to 27.1% for PHBV/WSF, and to 32.3% for PHBV/T. The obtained results correspond with the obtained values of X_c for PLA composites reinforced with silica/lignin hybrid fillers [43] and for PLA filled with cellulose nanofibrils, where cellulose-based nanoparticles were found to be heterogeneous nucleation sites for PLA crystallization [45]. The increase in X_c parameter suggests that the examined biofillers acted as nucleating agents for PHBV because of their large surface areas and high total volume of pores. However, a confirmation of this hypothesis requires some additional research.

Water Absorption of PHBV and its Composites

The percentage increase in sample mass during the water absorption process is shown in Fig. 8. For all composites, the percentage of mass increased with the increased incubation time in the water. Neat PHBV, PHBV/ESF, and PHBV/T composites had a similar mass of absorbed water. PHBV samples filled with WSF showed the highest water absorption (4.94%). Also, the addition of fillers containing lignocellulose increased the ability of the composites to absorb

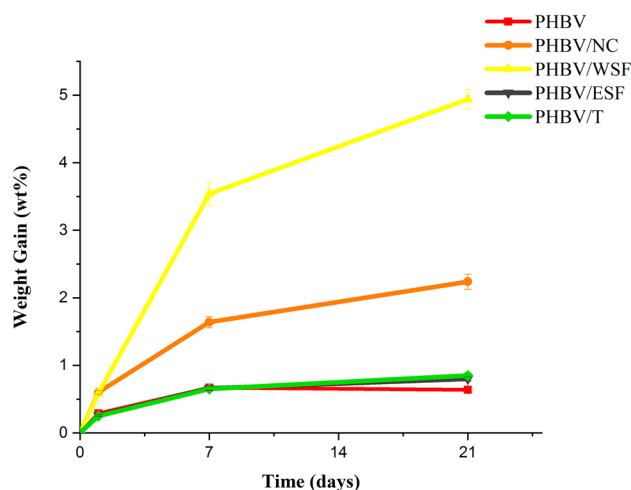


Fig. 8 Percent weight gain from water absorption for PHBV and its composites

Table 5 Mechanical properties of the neat PHB and composites after immersion in water

Symbol	σ [MPa]		E[MPa]	
	23 °C	21 days in water	23 °C	21 days in water
PHBV	7.6 ± 0.01	6.36 ± 0.017	382 ± 55	340 ± 48
PHBV/NC	7.9 ± 0.05	5.28 ± 0.084	607.2 ± 85	467 ± 18
PHBV/WSF	6.5 ± 0.03	1.21 ± 0.068	621 ± 12	317 ± 38
PHBV/ESF	7.3 ± 0.02	3.71 ± 0.004	411 ± 63	340 ± 16
PHBV/T	6.2 ± 0.16	4.61 ± 0.018	485 ± 42	394 ± 86

water. Similar results were obtained by Badia et al. [46], who investigated water absorption and hydrothermal performance of PHBV/sisal biocomposites (10, 20, 30 wt.%), using three various temperatures of hydrothermal test (26, 36, 46 °C). The results showed a general increase of mass for higher fibre content from 2.499 ± 0.123 up to 6.227 ± 0.311 (46 °C). The increase of water absorption by means of incorporation of lignocellulosic to the plastic matrix is well-known [47]. This filler consists of hygroscopic substances such as carbohydrates and lignin, which lead to an increased water uptake.

What can be observed for neat PHBV and composites filled with mineral particles, the stabilization of mass change and its decrease was noted, which was probably caused by the beginning of hydrolytic degradation.

Table 5 shows the values of strength properties obtained in a static tensile test after 21 days of samples' incubation in water. The tensile strength of the samples decreased after their incubation in water for 21 days, which indicated an enhanced rate of hydrolytic degradation. Higher decrease in tensile properties was observed for the composites containing the fillers of larger in size, such as WSF 82% or

ESF 49%, where water penetrates deep into the composite and accelerates degradation, at the same time reducing the mechanical properties. In that case, hydrolytic degradation negatively affects the modulus of elasticity to a lesser extent than the tensile strength, which likely results from a degradation process, in which polymer chain breakage and depolymerization occur before breaking up, resulting in brittleness.

Biodegradation of PHBV and its Composites

Figure 9 shows the mass percent of weight change for neat PHBV and its composites immersed in the compost heap. Improving the matrix with natural fillers accelerated the biodegradation process as compared to neat PHBV. Both the type and the size of the filler influence the material

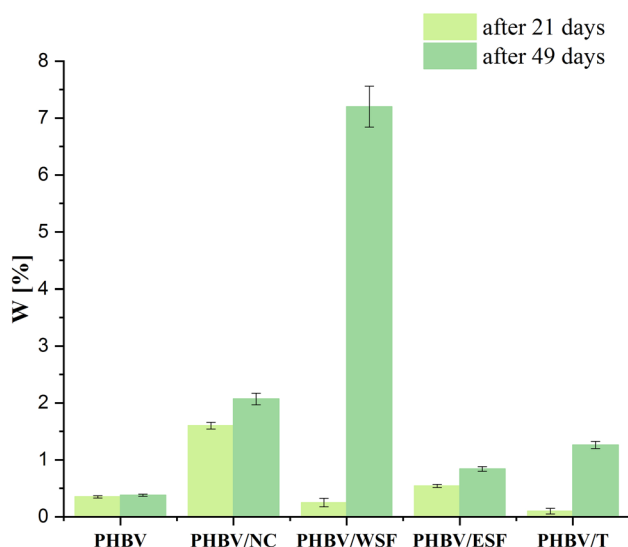


Fig. 9 Weight gain percentages of PHBV and its composites

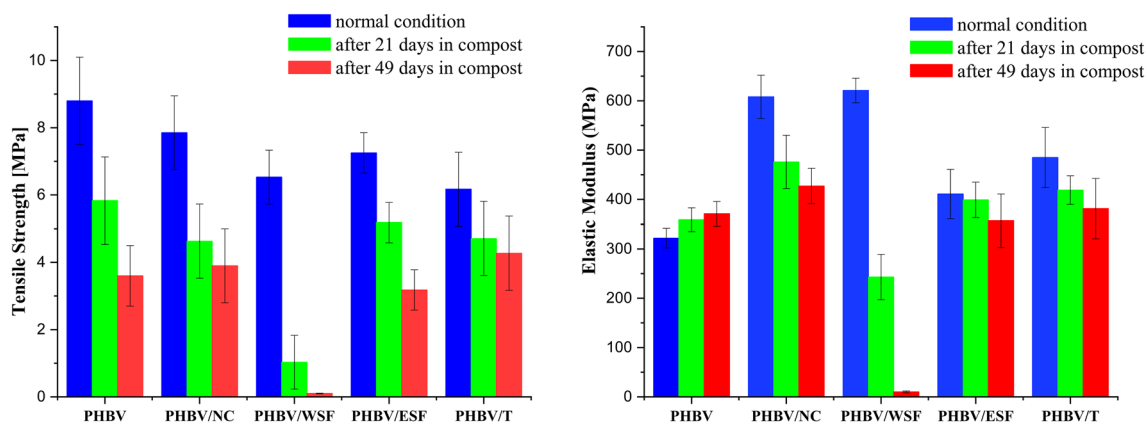


Fig. 10 Tensile strength and modulus of elasticity for PHBV and its composites immediately after injection, after 21 days in compost and after 49 days in compost

decomposition process. As in the case of water absorption, the high mass increase (over 7%) was exhibited by PHBV/WSF composites. Increase in mass was also noted for the PHBV/NC composites, whereby the highest increase occurred until the 21st day of incubation. Both composites containing lignocellulose fillers (WSF and NC) showed a higher mass increase due to the absorption of water contained in the compost. Mineral fillers such as for ESF caused a slight increase in weight 0.84% after 49 days.

Figure 10 shows the results of the tensile strength and modulus of elasticity of the tested composites immediately after injection, and after 21 and 49 days in compost. For all the tested samples, a decrease in the strength properties was observed with time, which was most pronounced after 49 days of storage in compost. A decrease in strength properties was caused by the progressive biodegradation of materials, which most probably resulted in the cracking of polymer chains [48]. The largest decrease was observed for PHBV/WSF after 49 days in compost, where tensile strength was close to 0. This result was most likely caused by the fact that the filler contained lignocellulose and had larger particles, which were easily disintegrated under composting conditions. Composites containing mineral fillers and NC particles (~3.76 MPa) exhibited a reduction in strength properties comparable to those found in the neat polymer (3.6 MPa). Changes in modulus of elasticity due to composting were lower than the changes in tensile strength due to the fact that stiffness had increased in the first step of biodegradation for neat PHBV.

The results of a bending test of neat PHBV and its examined composites at room temperature and after 21 and 49 days in compost are shown in Table 6. For the neat PHBV, changes under composting conditions were not high. After 21 days in the compost, both bending stresses and the modulus are in the same level for the composites, with the exception of PHBV/WSF, where a threefold decrease

Table 6 Mechanical properties of the neat PHB and composites after 21 and 49 days in compost

Symbol	σ [MPa]			E[MPa]		
	23 °C	21 days in compost	49 days in compost	23 °C	21 days in compost	49 days in compost
PHBV	13.4±0.03	13.0±0.02	9.6±0.22	333±0.02	299±0.005	272±0.09
PHBV/NC	12.5±0.02	10.9±0.25	8.0±0.08	464±0.04	455±0.005	356±0.002
PHBV/WSF	11.4±0.02	3.65±0.29	1.5±0.18	412±0.08	181±0.68	87
PHBV/ESF	11.3±0.16	10.7±0.04	7.3±0.10	333.5±0.10	322±0.08	295±0.01
PHBV/T	13.2±0.00	11.6±0.04	8.5±0.08	408.5±0.01	411±0.09	311±0.01

in these properties was observed (from 11.4±0.02 MPa to 1.5±0.18 MPa). The longer the composites remained in compost, the lower mechanical properties they exhibited. The largest decrease in properties was noted for the composites with lignocellulose fillers. A simple dependence between the size of filler particles and the biodegradation rate was also observed. This was due to the sorption of water over the phase boundaries and a greater absorption of water by large particles.

Conclusion

The addition of natural particles allows for tailoring the properties of composites based on the PHBV matrix, both in terms of achieving better strength properties and their faster biodegradation under special condition. The addition of natural fillers (either lignocellulose or mineral) increased the stiffness of the composites. The addition of natural particles accelerated the time of hydrolytic degradation and degradation in compost heap of the produced composites as compared to neat PHBV. The addition of biofillers to the PHBV matrix generally did not change the thermal stability of the biocomposites. A higher thermal stability was achieved only for the PHBV/NC. However, in each case, an increase in the degree of crystallinity calculated by means of scanning calorimetry was observed. Furthermore, larger crystallinity was caused by mineral particles rather than lignocellulosic particles.

Due to their short biodegradation time and lower environmental impact (biodegradability into water, carbon dioxide and biomass in soil and marine environments and non-toxicity) compared with petroleum-based polymers, composites based on PHBV with the addition of 15% of natural particles can therefore be used for production of wrapping or disposable materials, e.g. packaging for airline cosmetics, small boxes for vegetables, or sandwich packaging.

Acknowledgements The authors thank Dr. Iwona Cicha (University Hospital Erlangen) for the English language editing. This work was partly performed with the financial support from the Ministry of Science and Higher Education Grants 03/32/DSPB/0804—Poznan University of Technology.

Open Access This article is distributed under the terms of the Creative Commons Attribution 4.0 International License (<http://creativecommons.org/licenses/by/4.0/>), which permits unrestricted use, distribution, and reproduction in any medium, provided you give appropriate credit to the original author(s) and the source, provide a link to the Creative Commons license, and indicate if changes were made.

References

1. Elsayy MA, Kim KH, Park JW, Deep A (2017) Hydrolytic degradation of polylactic acid (PLA) and its composites. *Renew Sustain Energy Rev* 79:1346–1352. <https://doi.org/10.1016/j.rser.2017.05.143>
2. Pereira da Silva JS, Farias da Silva JM, Soares BG, Livi S (2017) Fully biodegradable composites based on poly(butylene adipate-co-terephthalate)/peach palm trees fiber. *Compos Part B Eng* 129:117–123. <https://doi.org/10.1016/j.compositesb.2017.07.088>
3. Rasal RM, Janorkar AV, Hirt DE (2010) Poly(lactic acid) modifications. *Prog Polym Sci* 35:338–356. <https://doi.org/10.1016/j.progpolymsci.2009.12.003>
4. Chen GQ, Jiang XR, Guo Y (2016) Synthetic biology of microbes synthesizing polyhydroxyalkanoates (PHA). *Synth Syst Biotechnol* 1:236–242. <https://doi.org/10.1016/j.synbio.2016.09.006>
5. Joyyi L, Ahmad Thirmizir MZ, Salim MS et al (2017) Composite properties and biodegradation of biologically recovered P(3HB-co-3HHx) reinforced with short kenaf fibers. *Polym Degrad Stab* 137:100–108. <https://doi.org/10.1016/j.polymdegradstab.2017.01.004>
6. Bledzki AK, Jaszkiwicz A (2010) Mechanical performance of biocomposites based on PLA and PHBV reinforced with natural fibres—a comparative study to PP. *Compos Sci Technol* 70:1687–1696. <https://doi.org/10.1016/j.compscitech.2010.06.005>
7. Faruk O, Bledzki AK, Matuana LM (2007) Microcellular foamed wood-plastic composites by different processes: a review. *Macromol Mater Eng* 21:256–262. <https://doi.org/10.1002/mame.20060406>
8. Dong W, Ma P, Wang S et al (2013) Effect of partial crosslinking on morphology and properties of the poly(β -hydroxybutyrate)/poly(d,l-lactic acid) blends. *Polym Degrad Stab* 98:1549–1555. <https://doi.org/10.1016/j.polymdegradstab.2013.06.033>
9. Pietrini M, Roes L, Patel MK, Chiellini E (2007) Comparative life cycle studies on poly(3-hydroxybutyrate)-based composites as potential replacement for conventional petrochemical plastics. *Biomacromol* 8:2210–2218. <https://doi.org/10.1021/bm0700892>
10. Orue A, Eceiza A, Arbelaz A (2018) Preparation and characterization of poly(lactic acid) plasticized with vegetable oils and reinforced with sisal fibers. *Ind Crops Prod* 112:170–180. <https://doi.org/10.1016/j.indcrop.2017.11.011>
11. Tawakkal ISMA, Cran MJ, Bigger SW (2014) Effect of kenaf fibre loading and thymol concentration on the mechanical and

- thermal properties of PLA/kenaf/thymol composites. *Ind Crops Prod* 61:74–83. <https://doi.org/10.1016/j.indcrop.2014.06.032>
12. Awal A, Rana M, Sain M (2015) Thermorheological and mechanical properties of cellulose reinforced PLA bio-composites. *Mech Mater* 80:87–95. <https://doi.org/10.1016/j.mechmat.2014.09.009>
 13. Sawpan MA, Pickering KL, Fernyhough A (2011) Improvement of mechanical performance of industrial hemp fibre reinforced polylactide biocomposites. *Compos Part A Appl Sci Manuf* 42:310–319. <https://doi.org/10.1016/j.compositesa.2010.12.004>
 14. Liu WJ, Yang HL, Wang Z et al (2002) Effect of nucleating agents on the crystallization of poly(3-hydroxybutyrate-co-3-hydroxyvalerate). *J Appl Polym Sci* 86:2145–2152. <https://doi.org/10.1002/app.11023>
 15. Dietrich K, Dumont MJ, Del Rio LF, Orsat V (2017) Producing PHAs in the bioeconomy—towards a sustainable bioplastic. *Sustain Prod Consum*. <https://doi.org/10.1016/j.spc.2016.09.001>
 16. Chan CM, Pratt S, Halley P et al (2019) Mechanical and physical stability of polyhydroxyalkanoate (PHA)-based wood plastic composites (WPCs) under natural weathering. *Polym Test* 73:214–221. <https://doi.org/10.1016/j.polymertesting.2018.11.028>
 17. Srubar WV, Pilla S, Wright ZC et al (2012) Mechanisms and impact of fiber-matrix compatibilization techniques on the material characterization of PHBV/oak wood flour engineered biobased composites. *Compos Sci Technol* 72:708–715. <https://doi.org/10.1016/j.compscitech.2012.01.021>
 18. Gunning MA, Geever LM, Killion JA et al (2013) Mechanical and biodegradation performance of short natural fibre polyhydroxybutyrate composites. *Polym Test* 32:1603–1611. <https://doi.org/10.1016/j.polymertesting.2013.10.011>
 19. Ke Y, Qu Z, Wu G, Wang Y (2014) Thermal and in vitro degradation properties of the NH₂-containing PHBV films. *Polym Degrad Stab* 105:59–67. <https://doi.org/10.1016/j.polymdegradstab.2014.03.039>
 20. Deroiné M, Le Duigou A, Corre YM et al (2014) Accelerated ageing and lifetime prediction of poly(3-hydroxybutyrate-co-3-hydroxyvalerate) in distilled water. *Polym Test* 39:70–78. <https://doi.org/10.1016/j.polymertesting.2014.07.018>
 21. Wu CS, Liao HT (2014) The mechanical properties, biocompatibility and biodegradability of chestnut shell fibre and polyhydroxyalkanoate composites. *Polym Degrad Stab* 99:274–282. <https://doi.org/10.1016/j.polymdegradstab.2013.10.019>
 22. Wu CS (2013) Preparation, characterization and biodegradability of crosslinked tea plant-fibre-reinforced polyhydroxyalkanoate composites. *Polym Degrad Stab*. <https://doi.org/10.1016/j.polymdegradstab.2013.04.013>
 23. Ryan CA, Billington SL, Criddle CS (2018) Biocomposite fiber-matrix treatments that enhance in-service performance can also accelerate end-of-life fragmentation and anaerobic biodegradation to methane. *J Polym Environ* 26:1715–1726. <https://doi.org/10.1007/s10924-017-1068-4>
 24. Tworzywa sztuczne - Oznaczenie właściwości mechanicznych przy statycznym rozciąganiu—Część 1: Zasady ogólne
 25. Bouzouita A (2016) Elaboration of polylactide-based materials for automotive application: study of structure-process-properties interactions Amani Bouzouita
 26. Rosa DS, Guedes CGF, Oliveira CM, Felisberti MI (2008) Processing and properties of mixtures of PHB-V with post-consumer LDPE. *J Polym Environ* 16:230–240. <https://doi.org/10.1007/s10924-008-0114-7>
 27. Tănase EE, Popa ME, Râpă M, Popa O (2015) PHB/cellulose fibers based materials: physical, mechanical and barrier properties. *Agric Agric Sci Procedia* 6:608–615. <https://doi.org/10.1016/j.aaspro.2015.08.099>
 28. Silverman T, Naffakh M, Marco C, Ellis G (2016) Morphology and thermal properties of biodegradable poly(hydroxybutyrate-co-hydroxyvalerate)/tungsten disulphide inorganic nanotube nanocomposites. *Mater Chem Phys* 170:145–153. <https://doi.org/10.1016/j.matchemphys.2015.12.032>
 29. Mirmehdi SM, Henrique G, Tonoli D et al (2017) Lignocellulose-polyethylene composite: influence of delignification, filler content and filler type. *Cellul Chem Technol Cellul Chem Technol* 51:341–346
 30. Tarverdi PK, Madoyan Z (2014) Preparation and properties of polypropylene and pa 6 composites reinforced with armenian tuff stone, vol. 2. European scientific institute, Archamps, pp. 161–166
 31. Gordobil O, Delucis R, Egüés I, Labidi J (2015) Kraft lignin as filler in PLA to improve ductility and thermal properties. *Ind Crops Prod* 72:46–53. <https://doi.org/10.1016/j.indcrop.2015.01.055>
 32. Elanchezhian C, Ramnath BV, Ramakrishnan G et al (2018) Review on mechanical properties of natural fiber composites. In: *Materials Today: Proceedings*. pp 1785–1790
 33. Sanjay MR, Arpitha GR, Yogesha B (2015) Study on mechanical properties of natural—glass fibre reinforced polymer hybrid composites: a review. In: *Materials today: proceedings*
 34. El-Hadi A, Schnabel R, Straube E et al (2002) Correlation between degree of crystallinity, morphology, glass temperature, mechanical properties and biodegradation of poly (3-hydroxyalkanoate) PHAs and their blends. *Polym Test* 21:665–674. [https://doi.org/10.1016/S0142-9418\(01\)00142-8](https://doi.org/10.1016/S0142-9418(01)00142-8)
 35. Dörrstein J, Scholz R, Schwarz D et al (2018) Effects of high-lignin-loading on thermal, mechanical, and morphological properties of bioplastic composites. *Compos Struct* 189:349–356. <https://doi.org/10.1016/j.compstruct.2017.12.003>
 36. Singh S, Mohanty AK, Sugie T et al (2008) Renewable resource based biocomposites from natural fiber and polyhydroxybutyrate-co-valerate (PHBV) bioplastic. *Compos Part A Appl Sci Manuf* 39:875–886. <https://doi.org/10.1016/j.compositesa.2008.01.004>
 37. Abdelwahab MA, Flynn A, Chiou B, Sen et al (2012) Thermal, mechanical and morphological characterization of plasticized PLA-PHB blends. *Polym Degrad Stab* 97:1822–1828. <https://doi.org/10.1016/j.polymdegradstab.2012.05.036>
 38. Melo JDD, Carvalho LFM, Medeiros AM et al (2012) A biodegradable composite material based on polyhydroxybutyrate (PHB) and carnauba fibers. *Compos Part B Eng* 43:2827–2835. <https://doi.org/10.1016/j.compositesb.2012.04.046>
 39. Naffakh M, Marco C, Ellis G et al (2014) Novel poly(3-hydroxybutyrate) nanocomposites containing WS₂ inorganic nanotubes with improved thermal, mechanical and tribological properties. *Mater Chem Phys* 147:273–284. <https://doi.org/10.1016/j.matchemphys.2014.04.040>
 40. Erceg M, Kovačić T, Klarić I (2005) Thermal degradation of poly(3-hydroxybutyrate) plasticized with acetyl tributyl citrate. *Polym Degrad Stab* 90:313–318. <https://doi.org/10.1016/j.polymdegradstab.2005.04.048>
 41. dos Santos Rosa D, Calil MR, Fassina Guedes C das Rodrigues G TC (2004) Biodegradability of thermally aged PHB, PHB-V, and PCL in soil compostage. *J Polym Environ* 12:239–245. <https://doi.org/10.1109/TDEL.2012.6148530>
 42. Janigová I, Lacík I, Chodák I (2002) Thermal degradation of plasticized poly(3-hydroxybutyrate) investigated by DSC. *Polym Degrad Stab* 77:35–41. [https://doi.org/10.1016/S0141-3910\(02\)00077-0](https://doi.org/10.1016/S0141-3910(02)00077-0)
 43. Grzabka-Zasadnińska A, Klapiszewski Ł, Bula K et al (2016) Supermolecular structure and nucleation ability of polylactide-based composites with silica/lignin hybrid fillers. *J Therm Anal Calorim* 126:263–275. <https://doi.org/10.1007/s10973-016-5311-3>
 44. Sibeled Piedade C, Luis Claudio M (2013) Thermal properties and morphology of high-density polyethylene filled with coffee dregs.

- J Therm Anal Calorim 114:1–4. <https://doi.org/10.1007/s10973-013-3121-4>
45. Fujisawa S, Zhang J, Saito T et al (2014) Cellulose nanofibrils as templates for the design of poly(l-lactide)- nucleating surfaces. *Polymer* 55:2937–2942. <https://doi.org/10.1016/j.polymer.2014.04.019>
46. Badia JD, Kittikorn T, Strömberg E et al (2014) Water absorption and hydrothermal performance of PHBV/sisal biocomposites. *Polym Degrad Stab* 108:166–174. <https://doi.org/10.1016/j.polymdegradstab.2014.04.012>
47. Gil-Castell O, Badia JD, Kittikorn T et al (2013) Hydrothermal ageing of polylactide/sisal biocomposites. *Studies of water absorption behaviour and physico-chemical performance. Polym Degrad Stab* 108:212–222. <https://doi.org/10.1016/j.polymdegradstab.2014.06.010>
48. Lyu S, Untereker D (2009) Degradability of polymers for implantable biomedical devices. *Int J Mol Sci* 10:4033–4065. <https://doi.org/10.3390/ijms10094033>

Publisher's Note Springer Nature remains neutral with regard to jurisdictional claims in published maps and institutional affiliations.